Transformation of nonfunctional spinal circuits into functional states after the loss of brain input

G. Courtine, Y. P. Gerasimenko, R. van den Brand, A. Yew, P. Musienko, H. Zhong , B. Song , Y. Ao, R. Ichyama, I. Lavrov , R. R. Roy, M.V. Sofroniew, and V.R. Edgerton

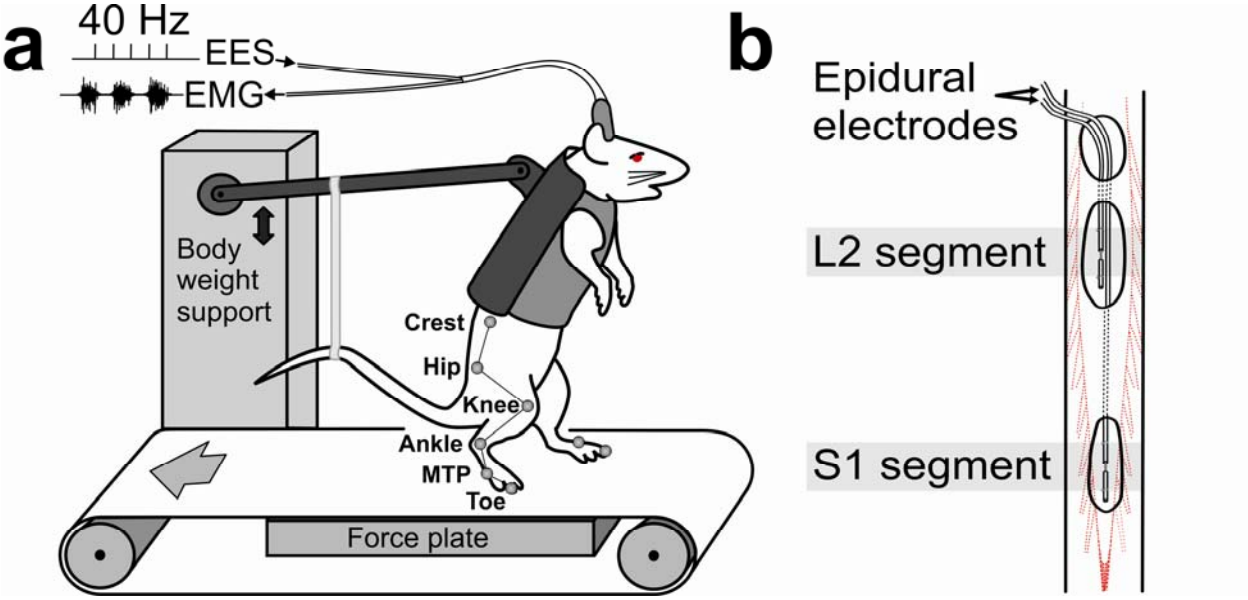

Supplementary Fig. 1: Experimental set up and epidural electrode implantation

a. The animal is positioned in an upper body jacket that is attached to a robotic arm that measures and controls the amount of weight support. Reflective markers are bilaterally attached to the shaved skin overlying bony landmarks to reconstruct 3-D hindlimb movements during stepping on the treadmill. Intramuscular and epidural electrodes are routed sub-cutaneously to a percutaneous amphenol head connector, enabling the recording of EMG activity and the delivery of electrical stimulation chronically. **b.** Wires are routed below the spinous processes and sutured over the dura on the dorsal aspect of L2 and S1 spinal segments. Stimulating electrodes are made by removing a small area (~1 mm notch) of the Teflon insulation on each wire.

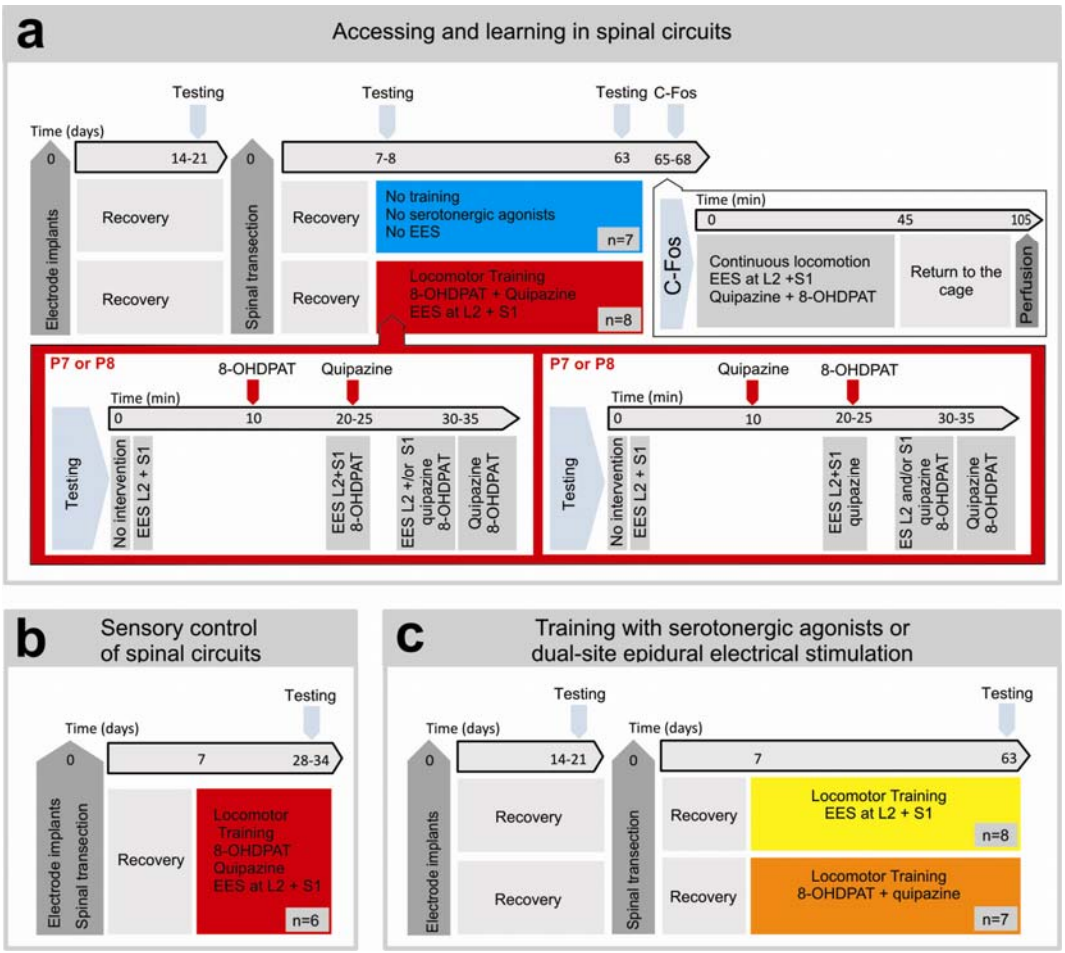

Supplementary Fig. 2: Timeline of the different experimental procedures

a. The ability of the pharmacological and electrical interventions to transform quiescent spinal locomotor circuits into functional states was tested at 7 and 8 days after a complete mid-thoracic spinal cord transection (n = 8). Spontaneous hindlimb movements in response to treadmill motion were recorded at the beginning of the testing session. The ability of EES to promote stepping was assessed afterwards. After these baseline recordings, quipazine or 8-OHDPAT was administrated systemically. Recordings of stepping ability were performed 10-15 min post-injection, and were immediately followed by the administration of quipazine or 8-OHDPAT. Locomotor recordings were conducted again 10-15 min after this second injection. Four rats received the first injection with quipazine on day 7 and with 8-OHDPAT on day 8. The other 4 rats were tested with the inverse sequence. No differences could be detected between the two sub-groups of rats. Data from day 7 were used to investigate the characteristics of locomotion under the combination of quipazine *plus* 8-OHDAPT and EES at L2 *plus* S1, as well as the effects of EES at L2 vs. S1. To assess any improvement with locomotor training, the same rats were trained for 8 weeks starting on day 8, after the completion of the experimental recordings. Another group of rats (n = 7) received no locomotor training and no pharmacological or EES interventions until the final testing day, 63 days post-lesion. In a terminal experiment, both non-trained rats and rats trained with the combination of interventions performed continuous treadmill locomotion for 45 min under the combination of quipazine *plus* 8-OHDAPT and EES at L2 *plus* S1. The rats were returned to their cages for I h and then killed. **b.** A group of 6 rats were trained for 3 weeks under the combination of quipazine plus 8-OHDAPT and EES at L2 plus S1. The ability of velocity-, load- and direction-dependent sensory input to modulate locomotor characteristics were evaluated in these animals at 28-34 days post-injury. c. Two groups of rats were trained under EES at L2 plus S1 or with quipazine plus 8-OHDPAT for 8 weeks. At the end of the training procedure, the locomotor ability of both groups of rats was tested under a combination of the interventions, as rats from (**a**)**.**

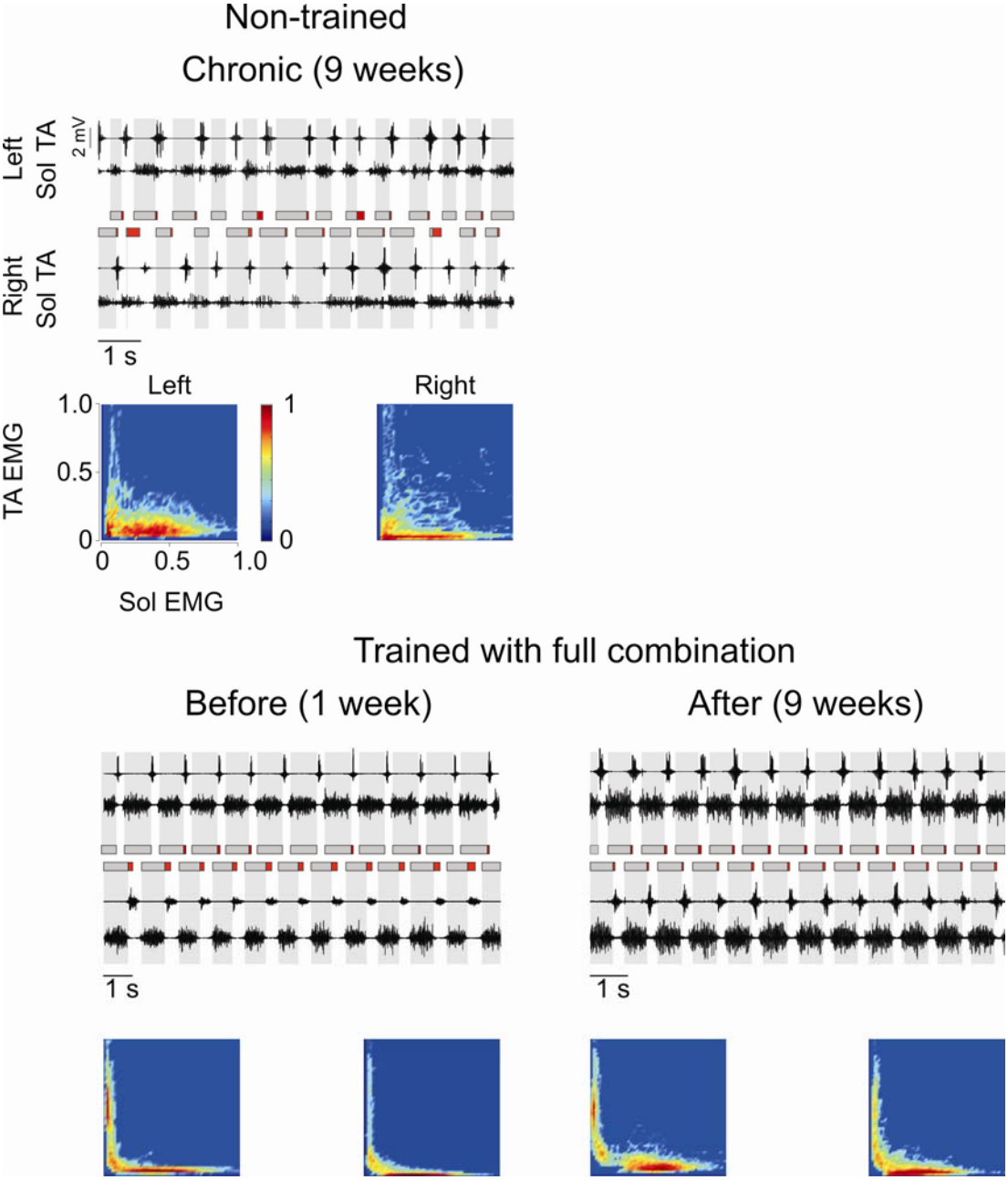

Supplementary Fig. 3: Coordination between the recruitment of extensor and flexor motor pools

A continuous sequence of treadmill stepping (9 cm/s) under EES at L2 and S1 recorded 15 min after the administration of quipazine and 8-OHDPAT is shown for a non-trained rat 9 weeks post-injury, and for a trained rat before (1 week) and after (9 weeks) chronic training. Raw EMG activity recorded in the Sol and TA muscles from both the left and right sides are displayed together with the durations of the stance (grey shaded) and drag (red shaded) phases. Probability density distributions of normalized EMG amplitudes in the Sol and TA muscles during treadmill stepping are shown at the bottom. L-shaped patterns observed during stepping sub-acutely and after locomotor training reveal reciprocal activation between the antagonist TA and Sol motor pools. Thickening of the L-shape during stepping of chronic non-trained rats indicates partial co-activation between the TA and Sol, i.e. loss of proper coordination between antagonist motor pools.

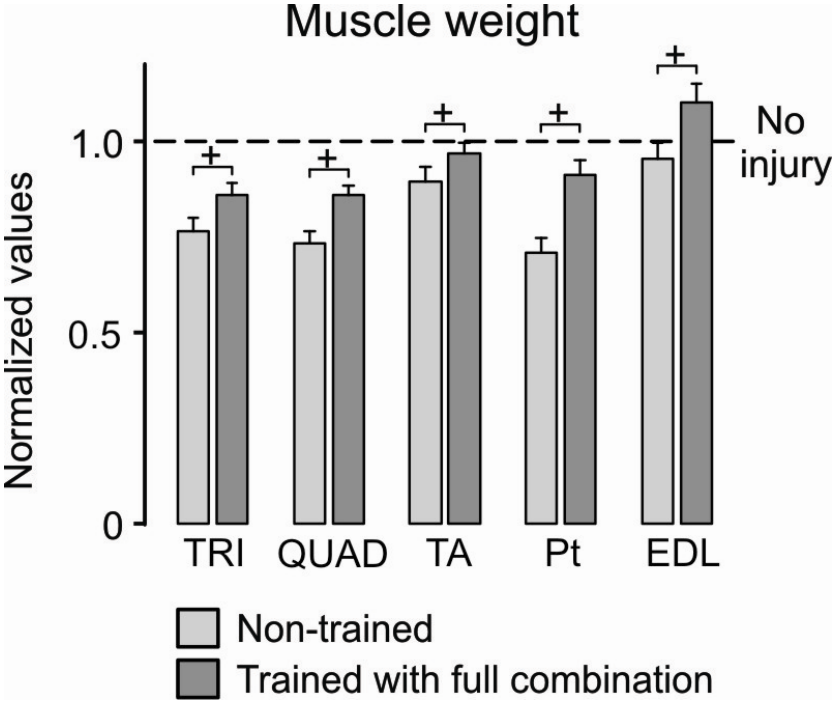

Supplementary Fig. 4: Post-mortem quantification of muscle weights

Bar graph of average values (n = 7 for non-trained, n = 8 for trained with a combination of the interventions) of normalized (to no injury rats, n = 5) muscle weights for triceps surae (soleus, medial gastrocnemius, lateral gastrocnemius), quadriceps (rectus femoris, vastus lateralis, vastus medialis, vastus intermedius), tibialis anterior, plantaris, and extensor digitorum longus muscles from the left hindlimb (see **Methods**). Error bars, S.E.M. Bars with a + sign link conditions that are significantly different ($p < 0.05$).

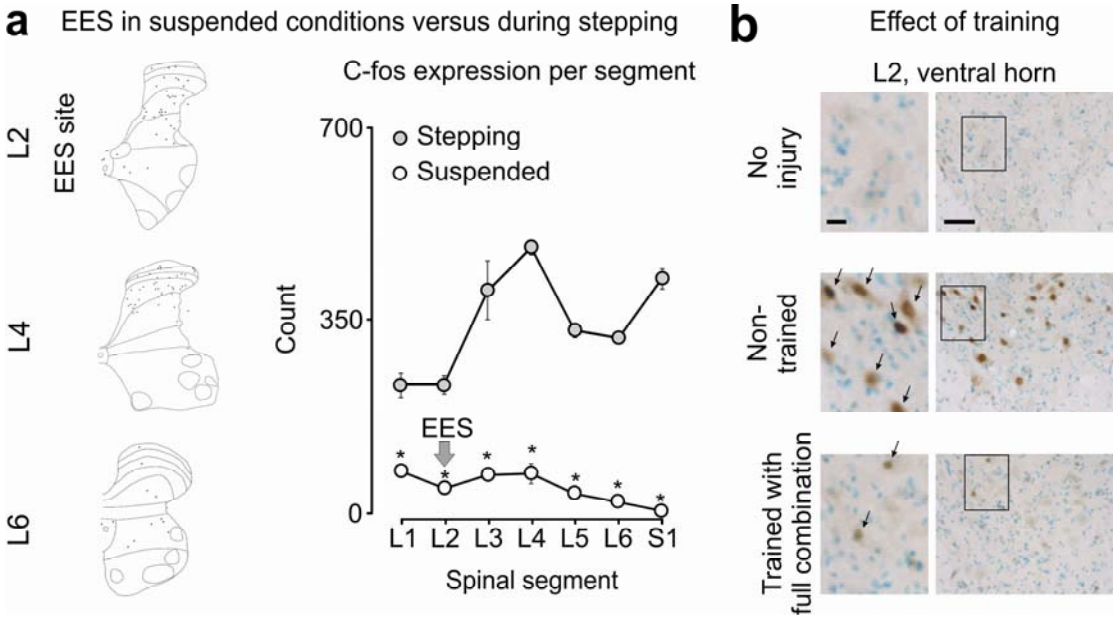

Supplementary Fig. 5: C-fos expression patterns

a. Representative example of camera lucida drawings of FOS+ cells in spinal segments L2, L4, and L6 induced by 45 min of continuous EES at L2 in a chronic non-trained spinal rat. EES at L2 without pharmacological stimulation did not induce air-stepping movements. Average values (open circle, n = 2) of total FOS+ cell count (all laminae) per spinal segment are shown together with average values (n = 5) measured following stepping under the full combination in non-trained spinal rats for comparison. In a suspended, non-weight bearing position, EES induced FOS expression in neurons located in laminae I-IV in the vicinity of the site of stimulation. Error bars, S.E.M. *, significantly different ($p < 0.01$) from values obtained during stepping. **b.** Representative example of FOS+ cells in the ventral aspect of the lumbar (L2) spinal cord for a non-injured rat and a non-trained spinal rat, as well as a spinal rat trained under the full combination. Scale bars, 100 µm and 50 µm for survey and detail images, respectively.

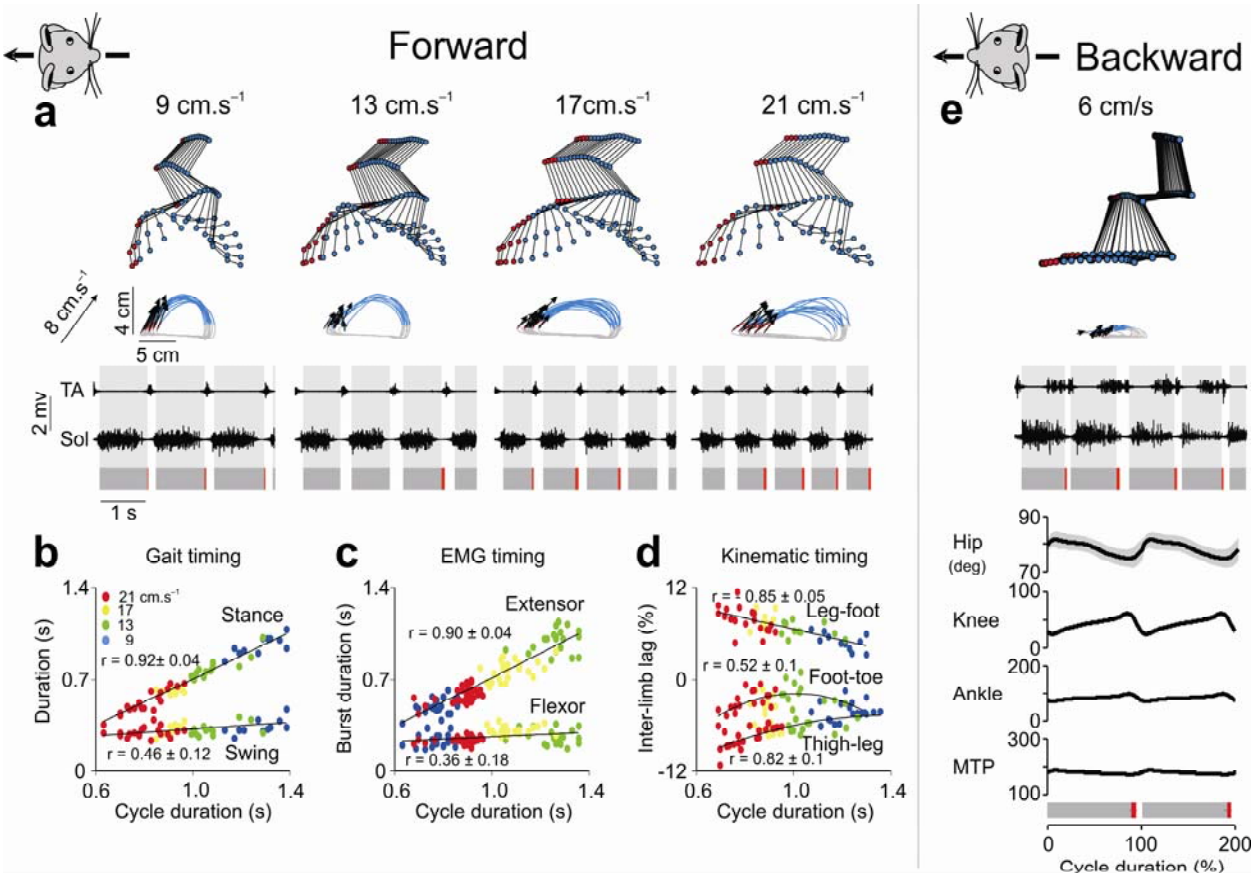

Supplementary Fig. 6: Sensory modulation of motor patterns in non-injured rats

a. Representative example of hindlimb kinematics and EMG activity recorded during locomotion on a treadmill at 9, 13, 17, and 21 cm.s^{-1} in non-injured rats. The actual treadmill belt speed is shown at the top of the graph. Conventions are the same as in **Fig. 6**, which reports the same data in spinal rats. **b.** The durations of the swing and stance phases are plotted against the cycle duration. Color-coded labels indicate the measured treadmill belt speed during the performance of the represented gait cycles. **c.** The durations of flexor (TA) and extensor (Sol) EMG bursts are plotted against the cycle duration. **d.** The temporal lag between oscillations (with respect to the direction of gravity) of adjacent hindlimb segments is plotted against the cycle duration. Inter-limb lags were computed by means of cross-correlation functions and expressed as a percent of cycle duration. Plots **a-d** are shown for a representative rat. Mean (± S.E.M) correlation values computed by averaging values obtained from linear regressions computed on each animal (n = 3 rats) individually are reported in each plot. **e.** Representative example of mean (+ one S.D.) hindlimb kinematics and raw EMG activity during continuous locomotion in the backward direction in a non-injured rat. Similar characteristics were observed in the other tested non-injured rats (n = 3). Conventions are the same as in **Fig. 8**, which reports the same data in spinal rats.

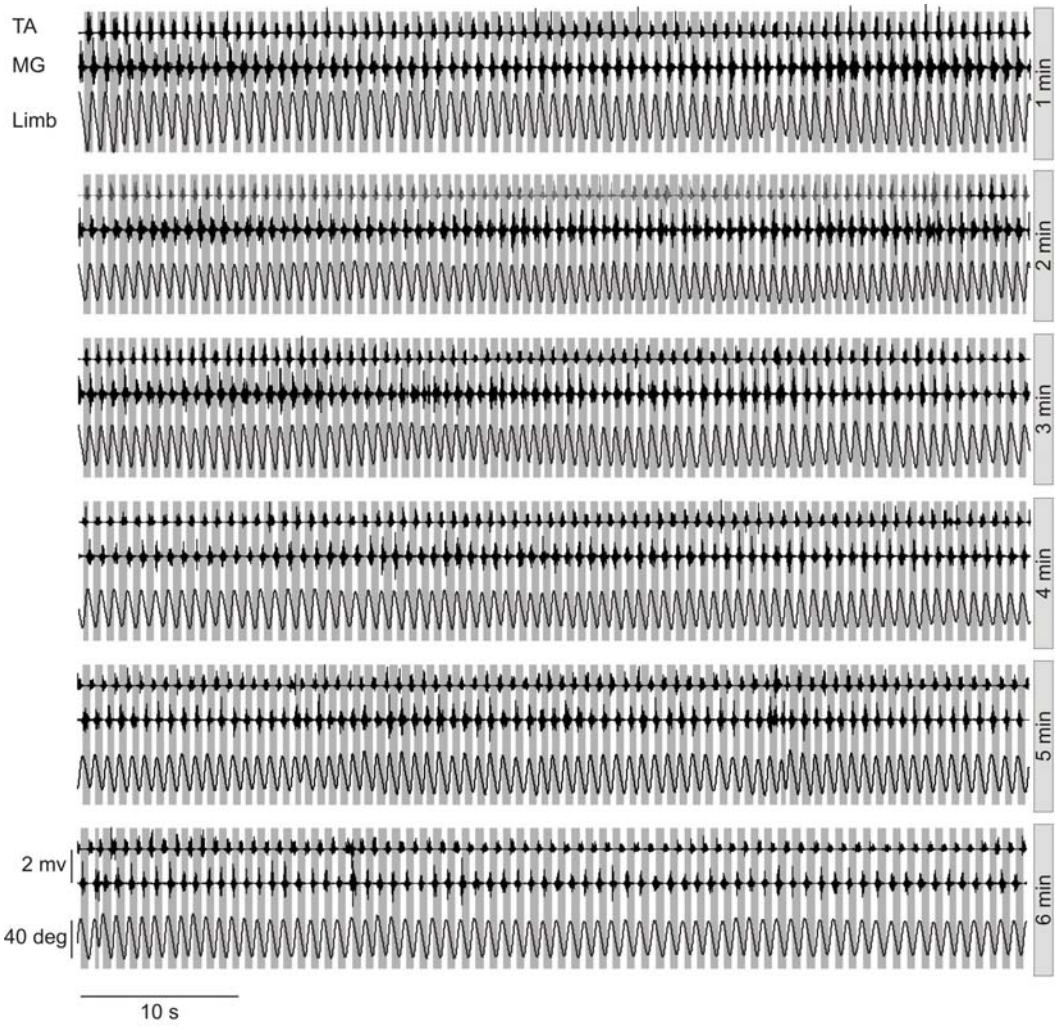

Supplementary Fig. 7: Continuous stepping at maximum stepping speed

A continuous sequence (6 min) of treadmill stepping (25 cm.s^{-1}) under EES at L2 *plus* S1 and quipazine *plus* 8-OHDPAT recorded 4 weeks post-injury is shown for a rat trained for 3 weeks (**supplementary Fig. 2b**). Raw EMG activity recorded in the MG and TA muscles are displayed together with the oscillations of the corresponding limb and the stance phase duration (grey boxes).

#	Gait timing
1	Cycle duration L
2	Cycle duration R
3	Stance duration L
4	Stance duration R
5	Swing duration L
6	Swing duration R
7	R value of cross correlation function between L-R limb oscillation
8	Variability Cycle duration L
9	Variability Cycle duration R
10	Variability of stance duration L
11	Variability of stance duration R
12	Variability of swing duration L
13	Variability of swing duration R
14	Variability of paw dragging duration L
15	Variability of paw dragging duration R

	Endpoint trajectory
16	Stride length L
17	Stride length R
18	Step height L
19	Step height R
20	Paw dragging duration L
21	Paw dragging duration R
22	Limb endpoint path length L
23	Limb endpoint path length R
24	Limb endpoint velocity vector orientation at swing onset L
25	Limb endpoint velocity vector orientation at swing onset R
26	Limb endpoint acceleration at swing onset L
27	Limb endpoint acceleration at swing onset R
28	Max limb endpoint velocity L
29	Max limb endpoint velocity R
30	Max backward limb endpoint position L
31	Max backward limb endpoint position R
32	Max forward limb endpoint position L
33	Max forward limb endpoint position R
34	Variability of Stride length L
35	Variability of Stride length R
36	Variability of step height L
37	Variability of step height R
38	Variability of limb endpoint path length L
39	Variability of limb endpoint path length R
40	Variability of limb endpoint velocity vector orientation L
41	Variability of limb endpoint velocity vector orientation R
42	Consistency of limb endpoint trajectory Sagittal L
43	Consistency of limb endpoint trajectory Sagittal R
44	Consistency of limb endpoint trajectory Vertical L
45	Consistency of limb endpoint trajectory Vertical R
46	Consistency of limb endpoint trajectory Medio-lateral L
47	Consistency of limb endpoint trajectory Medio-lateral R
48	Variability of limb endpoint acceleration at swing onset L
49	Variability of limb endpoint acceleration at swing onset R
50	Variability of max limb endpoint velocity L
51	Variability of max limb endpoint velocity R
52	Variability of max backward limb endpoint position L
53	Variability of max backward limb endpoint position R
54	Variability of max forward limb endpoint position L
55	Variability of max forward limb endpoint position R

	Joint angles
56	Hip joint extension L
57	Hip joint extension R
58	Hip joint flexion L
59	Hip joint flexion R
60	Hip joint amplitude L
61	Hip joint amplitude R
62	Knee joint extension L
63	Knee joint extension R
64	Knee joint flexion L
65	Knee joint flexion R
66	Knee joint amplitude L
67	Knee joint amplitude R
68	Ankle joint extension L
69	Ankle joint extension R
70	Ankle joint flexion L
71	Ankle joint flexion R
72	Ankle joint amplitude L
73	Ankle joint amplitude R
74	MTP joint extension L
75	MTP joint extension R
76	MTP joint flexion L
77	MTP joint flexion R
78	MTP joint amplitude L
79	MTP joint amplitude R

	Similitude with pre-lesion joint angles
80	Hip joint angle L
81	Hip joint angle R
82	Knee joint angle L
83	Knee joint angle R
84	Ankle joint angle L
85	Ankle joint angle R
86	MTP joint angle L
87	MTP joint angle R
88	Hip joint angular velocity L
89	Hip joint angular velocity R
90	Knee joint angular velocity L
91	Knee joint angular velocity R
92	Ankle joint angular velocity L
93	Ankle joint angular velocity R
94	MTP joint angular velocity L
95	MTP joint angular velocity R

	Joint angle variability
96	Variability of hip joint angle L
97	Variability of hip joint angle R
98	Variability of knee joint angle L
99	Variability of knee joint angle R
100	Variability of ankle joint angle L
101	Variability of ankle joint angle R
102	Variability of MTP joint angle L
103	Variability of MTP joint angle R

	Timing between joint angles
104	Hip-Knee correlation value L
105	Hip-Knee correlation value R
106	Knee-Ankle correlation value L
107	Knee-Ankle correlation value R
108	Ankle-MTP correlation value L
109	Ankle-MTP correlation value R

	Hindlimb oscillations
110	Limb axis amplitude L
111	Limb axis amplitude R
112	Mean limb axis velocity L
113	Mean limb axis velocity R

	EMG
114	EMG burst amplitude Soleus L
115	EMG burst amplitude Soleus R
116	EMG burst amplitude Tibialis Anterior L
117	EMG burst amplitude Tibialis Anterior R
118	EMG burst duration Soleus L
119	EMG burst duration Soleus R
120	EMG burst duration Tibialis Anterior L
121	EMG burst duration Tibialis Anterior R
122	Relative EMG burst onset Soleus L
123	Relative EMG burst onset Soleus R
124	Relative EMG burst onset Tibialis Anterior L
125	Relative EMG burst onset Tibialis Anterior R
126	Relative EMG burst end Soleus L
127	Relative EMG burst end Soleus R
128	Relative EMG burst end Tibialis Anterior L
129	Relative EMG burst end Tibialis Anterior R
130	Cross correlation L-R Soleus EMG

	Stability
131	Stance width L
132	Stance width R
133	Variability of pelvis oscillations in the sagital plane
134	Variability of pelvis oscillations in the medio-lateral plane

	Weight bearing capacities
135	Minimum body weight weight support

Supplementary Table 1: Summary of computed kinematics and EMG parameters

A total of 135 parameters were computed based on kinematics and EMG data recorded from the left (L) and right (R) hindlimbs during treadmill stepping. Variability in the parameters was computed, for each rat independently, as coefficients of variation (CV). The number (#) associated with each variable corresponds to their respective position in the representation of the PC analysis in **Fig. 1** and **Fig. 4**.